Coadsorption of gold with chlorine on CeO_2 (111) surfaces: A first principles study*

Lu Zhan-Sheng(路战胜)[a], He Bing-Ling(赫丙玲)[b], Ma Dong-Wei(马东伟)[c], and Yang Zong-Xian(杨宗献)[a]†

[a] College of Physics and Electronic Engineering, Henan Normal University, Xinxiang 453007, China
[b] Department of Physics and Electronic Engineering, Xinxiang University, Xinxiang 453003, China
[c] School of Physics, Anyang Normal University, Anyang 455000, China

(Received 14 April 2014; revised manuscript received 23 August 2014; published online 10 December 2014)

To investigate the effects of chlorine on the Au/ceria catalysts, the adsorption of gold or chlorine and their coadsorpiton on the stoichiometric and partially reduced CeO_2 (111) surfaces are studied from the first principles. It is found that the adsorption of Au is significantly enhanced by the chlorine preadsorption on the stoichiometric CeO_2 (111) surface; while on the partially reduced CeO_2 (111) surface, the preadsorbed chlorine inhabits the oxygen vacancy (which is the preferred adsorption site for gold), leading to a CeOCl phase and the dramatical weakening of the Au adsorption. Therefore, chlorine on the CeO_2 (111) surface can affect the Au adsorption thus the activity of the Au/CeO_2 catalyst.

Keywords: Au adsorption, chlorine, CeO_2 (111), first principles study

PACS: 68.35.–p, 71.15.Mb, 71.15.Nc, 71.20.–b **DOI:** 10.1088/1674-1056/24/2/026801

1. Introduction

CeO_2-supported Au catalysts have attracted much attention both from the experimental and theoretical researchers, owing to their super-catalytic activities for the low-temperature CO oxidation[1,2] and water-gas-shift (WGS) reactions,[3] as well as preferential CO oxidation (PROX).[4,5] To figure out these unusual properties, detailed knowledge of Au structures on ceria is undoubtedly of great importance. A lot of efforts have been made to find the plausible Au structures on ceria,[6–11] aiming to elucidate the microscopic origin of high catalytic activities found in experiments. The most studied ceria supports are the CeO_2 (111) surfaces with and without (O or Ce) vacancies. According to these studies, the Au atoms adsorbed at the O or Ce vacancies present high catalytic activities toward the CO oxidation or WGS reactions.[6,7,12,13] However, based on the first-principles thermodynamic analysis, Zhang *et al*. concluded that under the realistic reaction conditions (such as WGS reaction) the O vacancy is energetically much more preferable than the Ce vacancy.[14] Thus it is possible that Au atoms around the O vacancies are responsible for the high catalytic activities for CO oxidation and WGS reactions, as suggested by relevant experimental studies.[15–17]

In realistic experimental environments, the oxide surfaces will be covered with certain radicals, which can change the oxidation conditions of the support, and thus the activity turns towards metal adsorption.[18–21] Compared with the Au-nanoparticle catalysts, one of such radicals is hydroxyl, which can be envisaged to originate from the Au precursors or the air at moderate temperature.[20,22,23] Both experimental and theoretical studies have indicated the strong binding and positive charging of the interfacial Au atoms due to the decorated hydroxyl on the surfaces of the most studied oxides, such as TiO_2 and MgO.[18,20] Another electron–acceptor radical is chlorine, whose presence can also be ascribed to the Au precursors ($HAuCl_4$), especially in the conventional impregnation (IM) route.[24,25] Haruta, *et al*.[26] pointed out that due to the residual chlorine, the mean diameter of Au particles by IM is 10 times larger than that prepared by deposition precipitation (DP) and one of the most acceptable operations to produce highly active nano-gold catalyst is to completely remove chlorine.[27] Studies have found that residual chlorine displays negative effects on the Pt/CeO_2,[28] Au/CeO_2,[25] and Ir/CeO_2[29] catalysts, respectively. The effects of Na and Cl coadsorption on CO oxidation over MgO-supported Au nanoparticles have been studied by Broqvist *et al*.[30] It is found that Cl has a long-ranged characteristic effect as a poison, making both the adsorption of O_2 and the formation of the CO–O_2 intermediate complexes that mediate the formation of CO_2 more difficult. However, Zhang *et al*.[31] have shown that the controllable preparation of active Au/Fe_2O_3 catalyst can be achieved by using chlorine as an indicator, and that the active catalysts were prepared from solutions containing 2-ppm chlorine. Thus, up to now, the effect of chlorine on the Au/ceria catalyst is still unclear and theoretical investigations

*Project supported by the National Natural Science Foundation of China (Grant Nos. 11174070, 51401078, and 11147006), the China Postdoctoral Science Foundation (Grant No. 2012M521399), the Postdoctoral Research Sponsorship in Henan Province, China (Grant No. 2011038), and the Foundation for the Key Young Teachers of Henan Normal University and Start-up Foundation for Doctors of Henan Normal University, China.

†Corresponding author. E-mail: yzx@henannu.edu.cn

© 2015 Chinese Physical Society and IOP Publishing Ltd

are scarce. In the present work, the coadsorption of gold with chlorine on CeO_2 (111) surfaces is investigated to understand the effect of chlorine on the Au/ceria catalyst.

The rest of this paper is organized as follows. The computational details are presented in Section 2. The adsorptions of the Au atom, chlorine atom, and the coadsorption of Au and chlorine on the stoichiometric and partially reduced CeO_2 (111) surfaces are given in Section 3. Finally, some conclusions are drawn from the present study in Section 4.

2. Computational details

Spin-polarized Kohn–Sham density functional theory calculations are performed using the Vienna *ab initio* simulation package (VASP).[32–35] The electron exchange and correlation are treated within the generalized gradient approximation (GGA), using the Perdew–Burke–Ernzerhof (PBE) functional.[36] Since the conventional density function theory (DFT) based method is unable to describe the localization of the cerium 4f states of the partially reduced CeO_2, the Hubbard U parameter is introduced for the Ce 4f electrons to describe the on-site Coulomb interaction (the DFT + U method),[37,38] which helps to remove the self-interaction error and improves the description of correlation effects. In this work, the U parameter is set to be 5.0 eV, which is in agreement with many CeO_2 calculations in the literature and close to the value recommended by Castleton *et al.*[39] in their systematic exploration of the effect of the U value on the electron localization and structure of the partially reduced CeO_2. The Kohn–Sham orbitals are expanded by using plane waves with the well converged cut-off energy of 408 eV. The cerium 5s, 5p, 5d, 4f, 6s, the oxygen 2s, 2p, and the gold 5d, 6s electrons are treated as valence electrons. Brillouin-zone integrations are performed by using a 2×2×1 Monkhost–Pack grid and a Gaussion smearing parameter of SIGMA = 0.2 eV.

Ceria is an insulating rare-earth oxide. It has a cubic fluorite structure with four cerium and eight oxygen atoms per unit cell, and our calculations give an equilibrium lattice parameter of 5.480 Å. The optimized surface structure for the clean stoichiometric CeO_2 (111)-(3×3) supercell is shown in Figs. 1(a) and 1(b). The partially reduced CeO_2 (111) surface is represented by removing an oxygen atom from the top layer of the surface. Shapovalov and Metiu[13] have tested the convergence of the calculations with respect to the slab thickness and found that the six-layer slab provides converged surface (and adsorption) properties. Here we choose a slab thickness of six atomic layers for all calculations (two O–Ce–O stacks) with an in-plane periodicity of 3×3. During the optimization, three bottom atomic layers are fixed at their bulk positions to mimic the bulk, while the remaining ions are allowed to fully relax with a fixed cell based on the optimized lattice parameter for ceria bulk of 5.48 Å with the PBE functional.

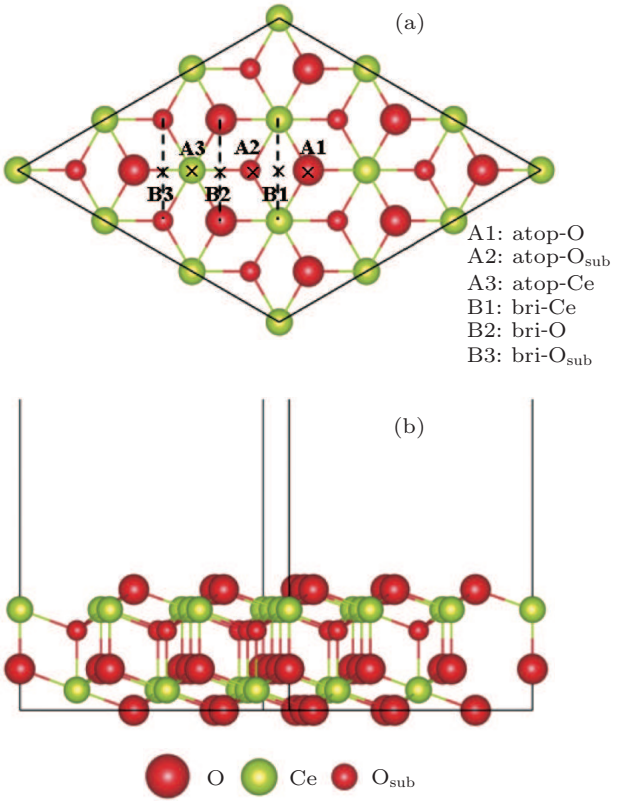


Fig. 1. (color online) Optimized surface structures: (a) top view and (b) side view for clean stoichiometric CeO_2 (111) with a 3×3 supercell. Here and in the following the "×" indicates the adsorption sites for Au or Cl, and red, light yellow, golden yellow, and green balls represent the O, Ce, Au, and Cl atoms, respectively. The abbreviation "bri" means bridge.

The adsorption energy of a gold or chlorine atom is evaluated on the $p(3\times3)$ supercells. The same supercells are used to study the coadsorption of a gold atom and a chlorine atom. The adsorption energy for an Au or a Cl atom is calculated as follows:

$$E^{\mathrm{ads}} = E^{\mathrm{tot}}_{\mathrm{subatrate}} + E^{\mathrm{tot}}_{\mathrm{Au(Cl)}} - E^{\mathrm{tot}}_{\mathrm{Au(Cl)-substrate}}. \quad (1)$$

The coadsorption of a gold atom and a chlorine atom is defined as

$$E^{\mathrm{coad}} = E^{\mathrm{tot}}_{\mathrm{substrate}} + E^{\mathrm{tot}}_{\mathrm{Au}} + E^{\mathrm{tot}}_{\mathrm{Cl}} - E^{\mathrm{tot}}_{\mathrm{Au-Cl-substrate}}, \quad (2)$$

where $E^{\mathrm{tot}}_{\mathrm{subatrate}}$ and $E^{\mathrm{tot}}_{\mathrm{Au(Cl)}}$ are the total energies of the substrate atom and the isolated atom (Au or Cl), respectively; $E^{\mathrm{tot}}_{\mathrm{Au(Cl)-substrate}}$ and $E^{\mathrm{tot}}_{\mathrm{Au-Cl-substrate}}$ are the total energies of the substrate with an Au atom or a Cl atom and both the Au and Cl atoms.

3. Results and discussion

3.1. Au adsorption on the stoichiometric and partially reduced CeO_2 (111) surface

Although much attention has been paid to the Au/CeO_2 (111) system, the energetically favorable adsorption configuration for the Au atom on the stoichiometric CeO_2 (111) surface is still controversial. Liu *et al.*,[6] Castellani *et al.*,[40]

and Chen *et al.*[3] pointed out that the favorable site for Au on stoichiometric CeO_2 (111) surface is the O-top site. However, Hernández *et al.*,[41] Camellone and Fabris,[12] Zhang *et al.*,[42] and Tang *et al.*[43] showed that the structure with Au on the O-bridge site has the largest adsorption energy. The disagreement may lie in the choice of the ultrasoft pseudopotentials and the method used to describe the valence electrons. Branda *et al.*[44] obtained two different stable adsorption sites at the Ce–O bridge and the O–O bridge from different methods. In our present work, adsorption of a single Au atom on the stoichiometric CeO_2 (111) surface is investigated at different trial adsorption sites, including atop-O, atop-Ce, atop-O_{sub} (subsurface oxygen), O-bridge and Ce-bridge sites, shown in Fig. 1(a). The adsorption data, including the optimized geometries, adsorption energies, spin moments, and the number of electrons transferred from the Au adatom on the stoichiometric surface are shown in Table 1. It is found that the Au atom prefers to bind with a surface oxygen atom with an adsorption energy of 1.14 eV and an Au–O distance of 2.01 Å. In terms of Bader charge analysis,[45] there is found a charge transfer of about 0.26*e* from Au to the substrate, thus Au loses a charge of 0.26*e*. The excess electrons are localized mainly on a nearest-neighboring (NN) surface Ce ion (denoted with a "#" as shown in Fig. 2(a)) with a spin moment of 0.83 μ_B.

Table 1. Optimized geometries, values of adsorption energy E_{ads}, (in eV), spin moment m (in μ_B), and the number of electrons q (in e) transferred from the Au adatom on the stoichiometric and partially reduced CeO_2 (111) surface. Positive and negative values of q mean losing and getting electrons, respectively. The same notations are adopted in Table 3.

Adsorption geometries	E_{ads}/eV	m/μ_B	$q(e)$
Au on the stoichiometric CeO_2 (111) surface			
atop-Ce	0.67	(Au) 0.61 (NNCe) 0.02 3(NNO) 0.05	(Au) –0.04
atop-O_{sub}	0.88	(Au) 0.32 3(NNO) 0.05	(Au) –0.07
bri-O_{sub}	1.04	(Au) 0.65 (NNCe) 0.05 (NNO) 0.15	(Au) –0.08 (NNO) +0.08
atop-O	1.14	(Au) 0.13 (Ce#) 0.83	(Au) +0.26 (Ce#) –0.20
Au on the partially reduced CeO_2 (111) surface			
O-vacancy (NNN Ce reduced)	2.73	(Ce#) 1.00	(Au) –0.58 (Ce#) –0.23

NN: nearest neighbor; 3(NNO): one of the three O atoms which are the nearest neighbors of the Au adatom.

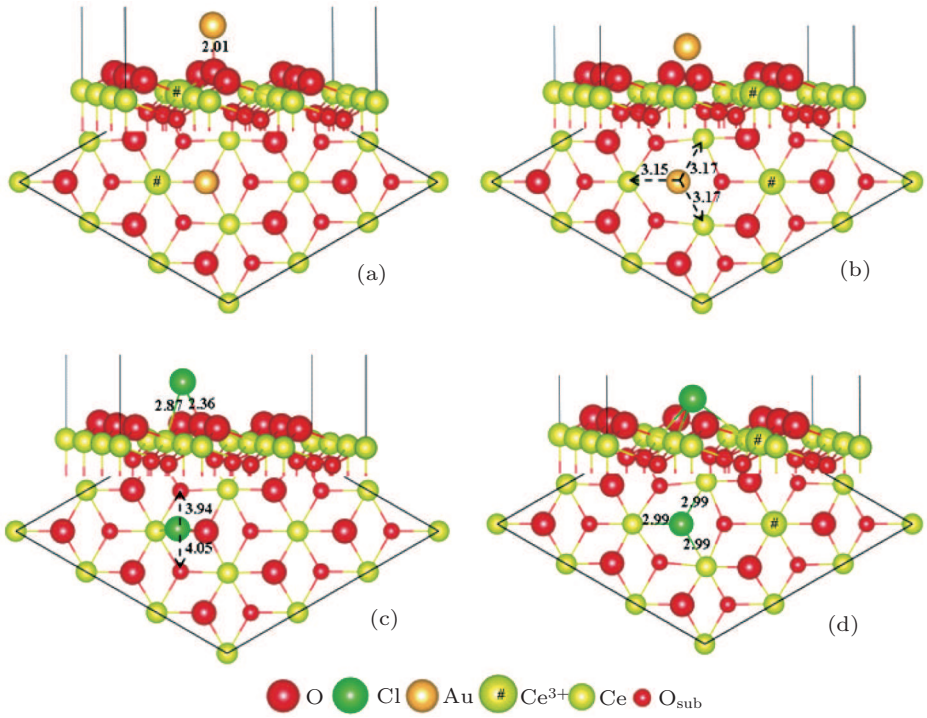


Fig. 2. (color online) The most stable optimized surface structures for an Au atom on the stoichiometric (a) and partially reduced (b) CeO_2 (111), and a Cl atom on the stoichiometric (c), and partially reduced (d) CeO_2 (111).

On the partially reduced CeO_2 (111) surface, we try different initial sites for the adsorption of an Au atom near the oxygen vacancy and the most stable geometry for the Au adatom is at the vacancy site as shown in Fig. 2(b) with the adsorption data shown in Table 1. In this structure, the Au atom is located at about 1.32 Å above the surface with respect to the surface O atoms and the adsorption energy is 2.73 eV. The adsorbed Au atom gains 0.58 *e*, and a next nearest-neighboring

(NNN) Ce ion is reduced to Ce^{3+} with a spin moment of 1.00 μ_B.

3.2. Cl adsorption on the stoichiometric and partially reduced CeO_2 (111) surface

The formation of a CeOCl phase under reaction conditions or during sample preparation treatments is experimentally verified in various catalytic systems, such as the reduction of the Rh(Cl)/CeO_2[46] and Pd(Cl)/CeO_2[47] catalysts, and the oxidation of HCl.[48,49] Experimentally, Vogtenhuber *et al.*[50] investigated chlorine adsorption on the rutile TiO_2 (110) surface, in combination with the *ab initio* method, and found that the O vacancy is the most active adsorption site. Ménétrey *et al.*[51] performed the DFT–GGA periodic calculations for Cl/MgO(110) and their results showed that the reduction of the surface allows a much stronger adsorption of Cl. Hu and Metiu[52] used the density functional theory to examine the dissociation of halogen molecules on CeO_2 (111), and showed that the Cl adatom in the stable structure on the stoichiometric CeO_2 (111) surface obtains 0.33 *e* from the substrate.

The investigated adsorption sites for a single Cl atom on the stoichiometric CeO_2 (111) surface are the same as those for the Au atom. The most stable optimized structure is shown in Fig. 2(c), which has an adsorption energy of 1.57 eV. The Cl adatom is adsorbed above the intersection of a surface O–Ce bridge and a subsurface O-bridge. The nearest neighboring distances of Cl–O and Cl–Ce are 2.36 Å and 2.87 Å, respectively. According to the calculated Bader charges,[45] Cl obtains about 0.36 *e* from the surface, while the NN O loses about 0.20 *e*. Our result is in good agreement with those in Ref. [52].

The most stable adsorption site for Cl on the partially reduced CeO_2 (111) surface is at the vacancy position, the same as that for Cl on the reduced TiO_2 (110)[50] or MgO(110).[51] The adsorption energy is 4.51 eV, with a CeOCl phase formed.[46,47] The optimized structure is shown in Fig. 2(d), where the Cl is located about 1 Å above the surface oxygen plane with the nearest neighboring Cl–Ce and Cl–O_{sub} distances of 2.99 Å and 3.26 Å∼3.31 Å, respectively. It is known that on the reduced CeO_2 (111) surface, corresponding to each oxygen vacancy, there are about 1.2 *e* excess electrons (left by the departed oxygen) localized on two Ce ions (Ce^{3+}). Upon the adsorption of the Cl on the oxygen vacancy, one of the Ce^{3+} is re-oxidized into Ce^{4+}. Bader analysis[45] shows that the Cl adatom on the vacancy obtains about 0.72 electrons (forming the Cl^-) from the surface and leaves the rest of the excess electrons localized mainly on an NNN Ce ion.

3.3. Coadsorption of Au with Cl on the stoichiometric CeO_2 (111)

To study the effects of the Cl species on the adsorption of Au, we try different adsorption sites for Au near the preadsorbed Cl adatom on the stoichiometric CeO_2 (111) surface.

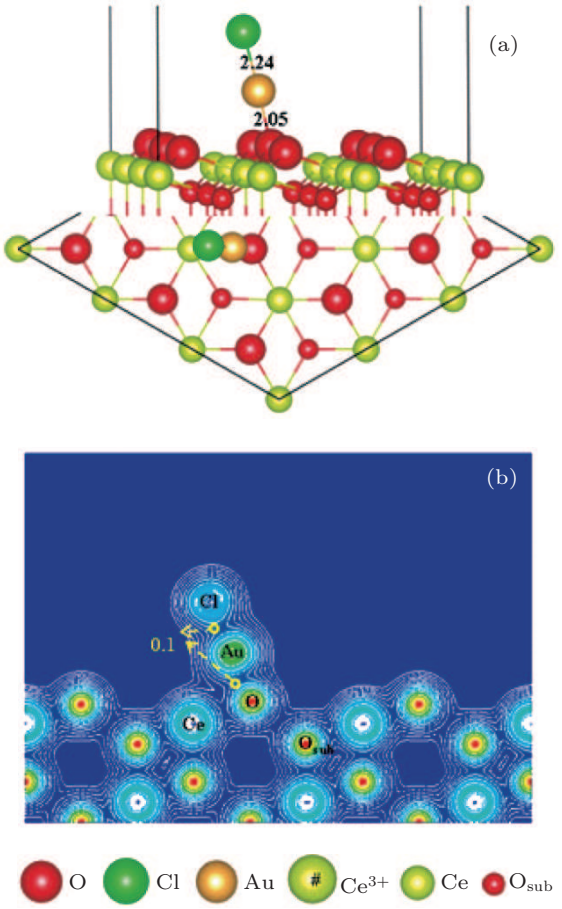


Fig. 3. (color online) The most stable optimized surface structures for Au and Cl coadsorption on the stoichiometric CeO_2 (111) (a), and its valence electron densities in the (110) plane (b). The electron-density contours start from 0.01 *e*/a.u.^{3} (a.u. is the abbreviation for atomic unit), and increase successively by a factor of $10^{1/5}$.

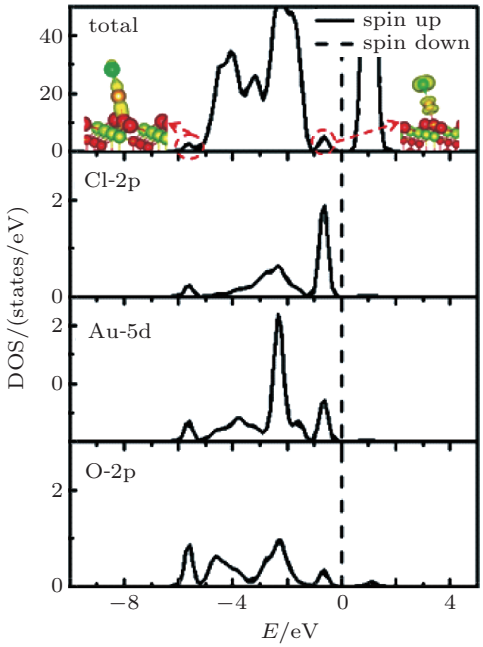


Fig. 4. (color online) The total density of states (TDOS) and local density of states (LDOS) for Au and Cl coadsorption on the stoichiometric CeO_2 (111) surface. The inserted figures are the corresponding figures for the two new peaks. The isosurface value is 0.02 *e*/a.u.^{3}

It is found that the Cl atom climbs up to the top of the Au atom with the bond lengths of 2.24 Å (Au–Cl) and 2.05 Å (Au–O), shown in Fig. 3(a). Au loses 0.26 *e*, and Cl gains 0.45*e*. The system converges to a nonmagnetic state with an enhanced adsorption energy of Au (3.73 eV) as compared with that on the pure stoichiometric surface (1.14 eV). The valence electron densities in the (110) plane, shown in Fig. 3(b), indicate that the Au atom bonds strongly with the Cl and O atoms. While, the charge transfer from Au to the substrate is independent of the presence of Cl. In order to find out the reason for the significant enhancement of the Au atom on the Cl preadsorbed CeO_2 (111) surface, we compare the structure and vibrational frequency of the adsorbed AuCl with those for the AuCl and $AuCl^-$ in a vacuum as shown in Table 2. Vibrational frequency calculations are performed for the AuCl through the numerical differencing of the atomic forces to generate a Hessian matrix. Diagonalization of the mass-weighted matrix gives rise to vibrational frequencies and atomic displacement vectors for the various modes. Only the atoms in the AuCl species are included in the vibrational analysis. The bond length (2.24 Å) and vibrational frequency (306 cm^{-1}) of the adsorbed AuCl structure are similar to those of the AuCl in a vacuum, i.e., a bond length of 2.22 Å and vibrational frequency of 366 cm^{-1}, which is in agreement with the experimental results[53] and previous calculated results.[54] From the total density of states (TDOS) curve (Fig. 4), we can see that two small peaks appear in energy ranges of −6.0 eV–5.3 eV and −1.0 eV–0 eV, respectively. The analysis from the local DOS (LDOS) shows that the new peaks are mainly due to Cl 2p, O 2p, and Au 5d, and the corresponding partial charge states are shown in the inserted figures in Fig. 4.

Table 2. Values of bond length d_{Au-Cl} (in Å) and frequency ω (in cm^{-1}) of the AuCl and $AuCl^-$ in a vacuum, as well as the adsorbed AuCl on the CeO_2 (111) surface.

	Experment[a]		Calculation[b]		This work		
	Neutral	Anion	Neutral	Anion	Neutral	Anion	Adsorbed
d_{Au-Cl}	2.20	2.35	2.22	2.43	2.22	2.42	2.24
ω	384	210	334	211	366	232	306

[a]Ref. [53]. [b]Ref. [54].

We also study the adsorption of a second Au atom on the CeO_2 (111) surface with and without Cl preadsorbed to investigate the effect of Cl on the Au congregation. The stable structure of two Au atoms on the CeO_2 (111) surface is shown in Fig. 5(a), with the bond lengths of 2.52 Å (Au–Au) and 2.09 Å (Au–O), respectively. There are about 0.1 *e* transferred from the surface O to the Au atoms.[55] The stable structure for the two Au on the CeO_2 (111) surface with Cl is shown in Fig. 5(b). The bond lengths are 2.03 Å (Au–O), 2.52 Å (Au–Cl), and 2.83 Å (Au–Au), respectively. The two Au atoms lose 0.60 *e*, Cl atom gains 0.33 *e*, and the excess electrons are localized on one of the NN Ce atoms. The adsorption energies of the second Au atom on the surface with and without Cl are 2.65 eV and 2.64 eV, respectively. Thus, although the preadsorbed Cl changes the adsorption site of the second Au atom, the effect on the adsorption energy is only about 0.01 eV. Owing to the significant enhancement of the first Au atom on the Cl preadsorbed CeO_2 (111) surface, the Cl adatom on the stoichiometric CeO_2 (111) may act as a nucleation site for the growth of the Au nanoparticles.

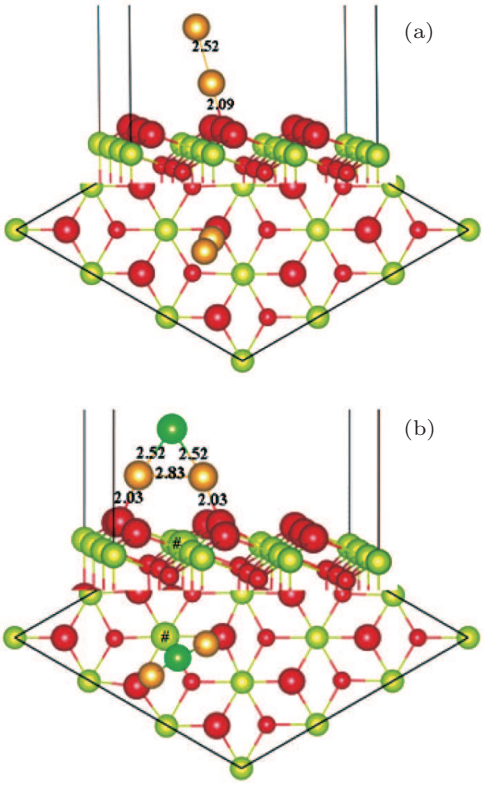


Fig. 5. (color online) The most stable optimized structures for two Au atoms on the stoichiometric CeO_2 (111) surface without (a) and with (b) Cl preadsorbed.

3.4. Coadsorption of Au with Cl on the partially reduced CeO_2 (111)

Our calculation results in Subsection 3.2 show that for Cl on the partially reduced CeO_2 (111) surface, the most stable adsorption site is on the oxygen vacancy and the CeOCl phase is formed. Here we investigate the adsorption of Au on the CeOCl. Different sites for Au (shown in Fig. 6) are considered, including the atop sites of Cl, O, O_{sub}, and Ce, as well as the bridge sites of O–O and O_{sub}–O_{sub}. The adsorption energies, spin moments, and the number of electrons transferred from the Au adatom on the CeOCl surface are shown in Table 3. It is found that the adsorption energies (0.22 eV–1.07 eV) of Au decrease dramatically compared with those on the stoichiometric CeO_2 (111) surface. The farther from the CeOCl site the Au atom is, the smaller influence it feels. In the optimized structure of Au on the Cl top as shown in Fig. 7(a), the adsorption energy is 0.22 eV with an Au–Cl distance of 2.56 Å, and Cl–Ce distances of 3.01 Å–3.04 Å, respectively.

From Bader charge analysis,[45] Cl and Au obtain 0.63 *e* and 0.06 *e*, respectively. The excess electron is still localized on an NNN Ce ion. The valence electron densities in the (110) plane are shown in Fig. 7(c), which indicates that the Au and Cl have a weak bonding. The most preferred adsorption site for Au on the CeOCl surface is still at the top site of a surface oxygen which is, at the same time, farthest from the Cl adsorption site (shown in Fig. 7(b)), where the Au is located about 2.00 Å above the surface oxygen atom. The adsorption energy is 1.07 eV with the Au losing 0.22*e* and the transferred electrons being localized on one NN Ce atom. Thus there are two Ce^{3+} atoms in this structure shown in Fig. 7(b). These results are close to those for Au on the stoichiometric CeO_2 (111). The three NN Cl–Ce bond lengths are 2.99, 2.99, and 3.00 Å, respectively, which are similar to those for Cl on the partially reduced CeO_2 (111).

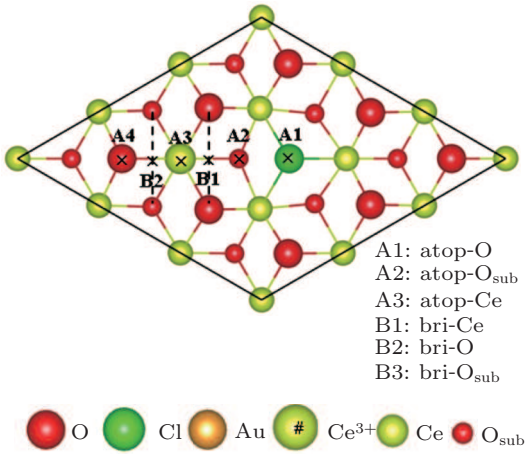


Fig. 6. (color online) Different trial adsorption sites for an Au adatom on the partially reduced CeO_2 (111) surface with Cl adsorbed.

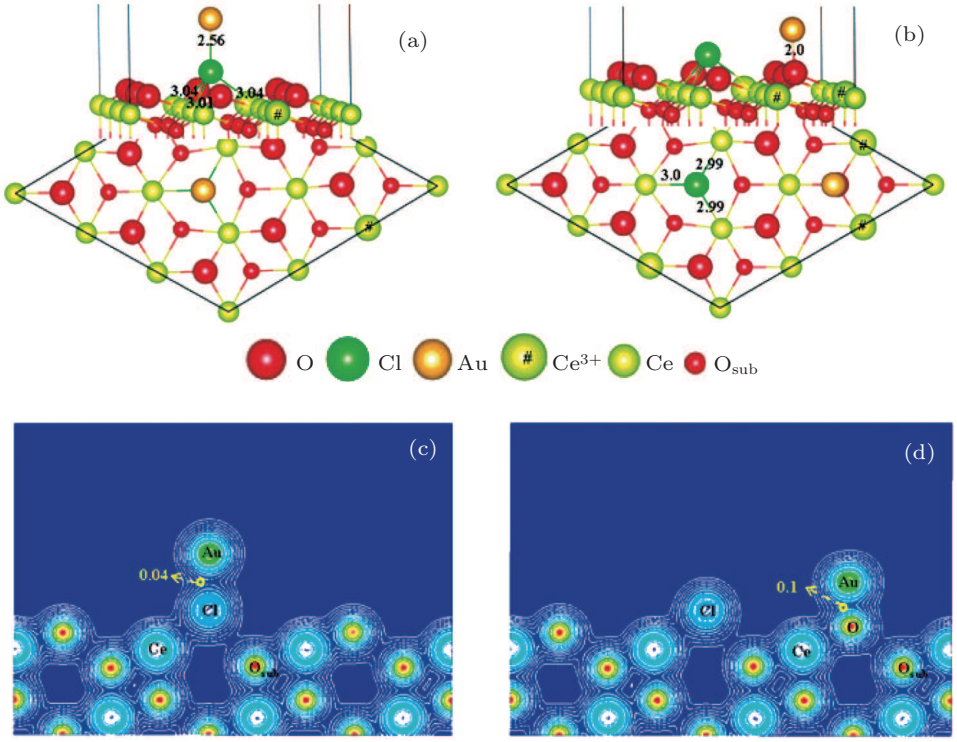


Fig. 7. (color online) Optimized surface structures of Au on the top of Cl (a) and surface oxygen (b) of the CeOCl (111) surface, as well as the valence electron densities in the (110) plane of (c) Au on Cl top and (d) Au on surface O top. The electron-density contours start from 0.01 *e*/a.u.^{3}, and increase successively by a factor of $10^{1/5}$.

Table 3. Optimized geometries, values of adsorption energy E_{ads} (in eV), spin moment m (in μ_B), and the number of electrons q (in e) transferred from the Au adatom on the partially reduced CeO_2 (111) surface with Cl adsorbed.

Adsorption geometries	E_{ads}/eV	m/μ_B	$q(e)$
atop-Cl	0.22	(Au) –0.76 (Cl) –0.10 (Ce#) 1.01	(Au) –0.06 (Cl) –0.63 (Ce#) –0.23
atop-O$_{sub}$	0.49	(Au) 0.53 (CeNNAu) –0.90	(Au) –0.1 (Cl) –0.66 (CeNNAu) -0.22
bri-O	0.46	(Au) –0.52 (CeNNAu) 0.75	(Au) –0.20 (Cl) -0.71 (CeNNAu) –0.17
atop-Ce#	0.47	(Au) 0.53 (CeNNAu) –0.72	(Au) –0.22 (Cl) –0.71 (CeNNAu) –0.17
bri-O$_{sub}$	unstable		
atop-O	1.07	(Au) –0.14 2(Ce#) –0.90	(Au) +0.22 (Cl) –0.72 2(Ce#) –0.20

NN: nearest neighbor; 2(Ce#): one of the two Ce# atoms; CeNNAu: the Ce atom which is the nearest neighbor of the Au adatom.

The total energies of the two systems: a Cl atom adsorbed on the top of the preadsorbed Au on the O vacancy and, inversely, an Au atom adsorbed on the top of the preadsorbed Cl on the O vacancy, show that the former is less stable (higher in energy by 0.13 eV) than the latter. Therefore, the Cl atoms prefer to occupy the oxygen vacancy sites. In Subsection 3.1, we have discussed that the most stable adsorption site for Au on the partially reduced CeO_2 (111) surface is on the oxygen vacancy. Thus Cl may occupy the O vacancy site, which will change the adsorption of Au.

4. Conclusions

The adsorptions of gold on the stoichiometric and partially reduced CeO_2 (111) surfaces with and without Cl preadsorption are studied by using the DFT + U method. It is found that the top of the surface oxygen atom and the oxygen vacancy are the preferred adsorption sites for Au on the stoichiometric and partially reduced CeO_2 (111) surface, respectively. The binding of Au to the partially reduced CeO_2 (111) is much stronger than that to the stoichiometric CeO_2 (111) surface. With the preadsorption of Cl on the stoichiometric CeO_2 (111) surface, the adsorption of Au is significantly enhanced by forming a structure of AuCl with Au on the surface and O and Cl above the Au adatom. On the partially reduced CeO_2 (111), the preadsorbed Cl inhabits the oxygen vacancy which is the preferred adsorption site for Au and leads to the formation of a CeOCl phase. The adsorption of Au on the Cl preadsorbed partially reduced CeO_2 (111) is much weaker as compared with that on the bare partially reduced CeO_2 (111). Our results indicate that the preadsorbed Cl adatom on the stoichiometric CeO_2 (111) may act as a nucleation site for the growth of the Au nanoparticles. However, Cl prefers to occupy the O vacancy sites on the partially reduced CeO_2 (111), which will affect the Au adsorption thus the activity of the Au/CeO_2 catalyst.

References

[1] Guzman J, Carrettin S and Corma A 2005 *J. Am. Chem. Soc.* **127** 3286
[2] Park E D 2006 *Studies in Surface Science and Catalysis* (Amsterdam: Elsevier) pp. 321–324
[3] Chen Y, Cheng J, Hu P and Wang H 2008 *Surf. Sci.* **602** 2828
[4] Avgouropoulos G, Papavasiliou J, Tabakova T and Idakiev V 2006 *T Ioannides Chem. Eng. J.* **124** 41
[5] Park E D, Lee D and Lee H C 2009 *Catal. Today* **139** 280
[6] Liu Z, Jenkins S J and King D A 2005 *Phys. Rev. Lett.* **94** 196102
[7] Zhang C, Michaelides A and Jenkins S J 2011 *Phys. Chem. Chem. Phys.* **13** 22
[8] Zhou Y, Lawrence N J, Wang L, Kong L, Wu T, Liu J, Gao Y, Brewer J R, Lawrence V K, Sabirianow R F, Soo Y, Zeng X, Dowben P A, Mei W and Cheung C L 2013 *Angew. Chem. Int. Ed.* **52** 6936
[9] Ghosh P, Camellone M F and Fabris S 2013 *J. Phys. Chem. Lett.* **4** 2256
[10] Longo A, Liotta L F, Pantaleo G, Giannici F, Venezia A M and Martorana A 2012 *J. Phys. Chem. C* **116** 2960
[11] Ta N, Liu J, Chenna S, Crozier P A, Li Y, Chen A and Shen W 2012 *J. Am. Chem. Soc.* **134** 20585
[12] Camellone M F and Fabris S 2009 *J. Am. Chem. Soc.* **131** 10473
[13] Shapovalov V and Metiu H 2007 *J. Catal.* **245** 205
[14] Zhang C, Michaelides A, King D A and Jenkins S J 2009 *J. Phys. Chem. C* **113** 6411
[15] Vindigni F, Manzoli M, Damin A, Tabakova T and Zecchina A 2011 *Chem.-Eur. J.* **17** 4356
[16] Tabakova T, Boccuzzi F, Manzoli M and Andreeva D 2003 *Appl. Catal. A: Gen.* **252** 385
[17] Lu J, Gao H, Shaikhutdinov S and Freund H J 2007 *Catal. Lett.* **114** 8
[18] Wang J and Hammer B 2006 *Phys. Rev. Lett.* **97** 136107
[19] Jiang D, Overbury S H and Dai S 2011 *J. Phys. Chem. Lett.* **2** 1211
[20] Brown M A, Fujimori Y, Ringleb F, Shao X, Stavale F, Nilius N, Sterrer M and Freund H J 2011 *J. Am. Chem. Soc.* **133** 10668
[21] Zhang R, Wang B, Liu H and Ling L 2011 *J. Phys. Chem. C* **115** 19811
[22] Moreau F, Bond G C and Taylor A O 2005 *J. Catal.* **231** 105
[23] Haruta M 2004 *J. New Mater. Electrochem. Systems* **7** 163
[24] Fu Q, Saltsburg H and Stephanopoulos M F 2003 *Science* **301** 935
[25] Arena F, Famulari P, Trunfio G, Bonura G, Frusteri F and Spadaro L 2006 *Appl. Catal. B-Environ.* **66** 81
[26] Haruta M 2002 *CATTECH* **6** 102
[27] Hugon A, Kolli N E and Louis C 2010 *J. Catal.* **274** 239
[28] Wootsch A, Descorme C, Duprez D 2004 *J. Catal.* **225** 259
[29] Huang Y, Wang A, Li L, Wang X and Zhang T 2010 *Catal. Comm.* **11** 1090
[30] Broqvist P, Molina L M, Grönbeck H and Hammer B 2004 *J. Catal.* **227** 217
[31] Zhang C, Liu L, Cui X, Zheng L, Deng Y and Shi F 2013 *Sci. Rep.* **3** 1503
[32] Kresse G and Hafner J 1993 *Phys. Rev. B* **47** 558
[33] Kresse G and Furthmüller J 1996 *Phys. Rev. B* **54** 11169
[34] Kresse G and Furthmüller J 1996 *Comput. Mater. Sci.* **6** 15
[35] Kresse G and Joubert D 1999 *Phys. Rev. B* **59** 1758
[36] Perdew J P, Burke K and Ernzerhof M 1996 *Phys. Rev. Lett.* **77** 3865
[37] Anisimov V I, Zaanen J and Andersen O K 1991 *Phys. Rev. B* **44** 943
[38] Dudarev S L, Botton G A, Savrasov S Y, Humphreys C J and Sutton A P 1998 *Phys. Rev. B* **57** 1505
[39] Castleton C W M, Kullgren J and Hermansson K 2007 *J. Chem. Phys.* **127** 244704
[40] Castellani N J, Branda M M, Neyman K M and Illas F 2009 *J. Phys. Chem. C* **113** 4948
[41] Hernández N C, Ricardo Grau-Crespo, Leeuw N H D and Sanz J F 2009 *Phys. Chem. Chem. Phys.* **11** 5246
[42] Zhang C, Michaelides A, King D A and Jenkins S J 2008 *J. Chem. Phys.* **129** 194708
[43] Tang Y, Zhang H, Cui L, Ouyang C, Shi S, Tang W, Li H and Chen L 2012 *J. Power Sources* **197** 28
[44] Branda M M, Hernaández N C, Sanz J F and Illas F 2010 *J. Phys. Chem. C* **114** 1934
[45] Henkelman G, Arnaldsson A and Jónsson H 2006 *Comput. Mater. Sci.* **36** 354
[46] Fajardie F, Tempere O, Manoli J M, Mariadassou G D and Blanchard G 1998 *J. Chem. Soc. Faraday Trans.* **94** 3727
[47] Kępiński L and Okal J 2000 *J. Catal.* **192** 48
[48] Farra R, Girgsdies F, Frandsen W, Hashagen M, Schlögl R and Teschner D 2013 *Catal. Lett.* **143** 1012
[49] Amrute A P, Mondelli C, Moser M, Leruth G N, López N, Rosenthal D, Farra R, Schuster M E, Teschner D, Schmidt T and Ramírez J P 2012 *J. Catal.* **286** 287
[50] Vogtenhuber D, Podloucky R, Redinger J, Hebenstreit E L D, Hebenstreit W and Diebold U 2002 *Phys. Rev. B* **65** 125411.
[51] Ménétrey M, Markovits A and Minot C 2004 *Surf. Sci.* **566** 693
[52] Hu Z and Metiu H 2012 *J. Phys. Chem. C* **116** 6664
[53] Evans C J and Gerry M C L 2000 *J. Mol. Spectrosc.* **203** 105
[54] Wu X, Xie H, Qin Z, Tan K, Tang Z and Lu X 2011 *J. Phys. Chem. A* **115** 6321
[55] Teng B, Wu F, Huang W, Wen X, Zhao L and Luo M 2012 *ChemPhysChem* **13** 1261